

Impact of temperature on the performance and fouling behavior of a forward osmosis membrane system for concentrating low-strength sewage

Nguyen Anh-Vu^a, Youhei Nomura^{a,b}, Taira Hidaka^{a,b}, Taku Fujiwara^{a,b,*}

^a Department of Environmental Engineering, Graduate School of Engineering, Kyoto University, Kyoto-Daigaku-Katsura, Nishikyo-ku, Kyoto 615-8540, Japan

^b Department of Global Ecology, Graduate School of Global Environmental Studies, Kyoto University, Kyoto-Daigaku-Katsura, Nishikyo-ku, Kyoto 615-8540, Japan

ARTICLE INFO

Editor: Ludovic F. Dumée

Keywords:

Forward osmosis
Organic recovery
Permeate flux
Solute rejection
Biodegradation

ABSTRACT

The forward osmosis (FO) process relies on the natural osmosis phenomenon, which is influenced by temperature through its effects on osmotic pressure and hydrodynamic properties. However, the impact of temperature on the FO membrane system for concentrating real sewage has not been clearly studied, with conflicting results reported. This study investigated the effects of temperature on the performance and fouling behavior of a laboratory-scale FO membrane system used to concentrate low-strength sewage with 1.2 M NaCl as the draw solution (DS). Permeate flux was found to increase notably with increasing temperature; however, it decreased by 30–40 % over 24 h due to membrane fouling. Additionally, while solute concentration efficiency improved with increasing temperature, particularly for nutrients, it remained lower than anticipated compared to the volume reduction ratio of the feed solution, which is attributable to solute accumulating within the fouling layers, diffusion into the DS, and degradation. Other notable observations include the heightened penetration of ammonia nitrogen into the DS with increasing temperature and the pronounced biodegradability of organic matter. Despite the observed drawbacks, the improved filtration performance, increased solute concentration, and mitigated fouling are significant findings, suggesting a path for optimizing future FO membrane filtration through temperature control.

1. Introduction

Forward osmosis (FO) membrane technology exploits the osmotic pressure difference between the two sides of a semi-permeable membrane, thereby driving water from the feed solution (FS) to the draw solution (DS). Here, the semipermeable membrane serves as a barrier to solutes and particles and should enable only water molecules to traverse. By requiring minimal hydraulic pressure, FO offers numerous advantages over conventional membrane methods, including lower energy consumption, low membrane fouling risks, simplified membrane cleaning, and enhanced filtration efficiency and water recovery [1]. The versatility of FO membranes extends their applicability to diverse industries, including water and wastewater treatment, manufacturing, food and beverage processing, the chemical and pharmaceutical sectors, and agriculture [1–4]. FO membrane utility includes various functions, such as desalination, material recovery, concentration, dilution, and even drug delivery and electricity generation applications.

Several factors intricately affect the performance and operation of an

FO membrane system, with temperature assuming a pivotal role owing to its direct relationship with osmotic pressure. According to van't Hoff equation [5], osmotic pressure is proportional to both temperature and concentration, with osmotic pressure increasing with temperature and more noticeable increments observed in more concentrated solutions. Therefore, a DS with a substantially higher concentration experiences a more significant increase in osmotic pressure than the FS at elevated temperatures, leading to a greater osmotic pressure difference between the two solutions. Meanwhile, the solution-diffusion model [6,7] reveals that the osmotic pressure difference drives trans-membrane permeate flux, suggesting a direct effect of temperature on permeate flux. Additionally, elevating temperature typically reduces viscosity, increases solubility, and enhances diffusivity, thereby facilitating mass transfer; it is also believed to trigger thermal expansion of the membrane, widening its pores and allowing greater molecular passage. Consequently, permeate flux and reverse solute flux (RSF) are hypothesized to increase with rising temperature, while membrane selectivity diminishes, leading to solute loss from the FS to the DS and vice versa. Higher

* Corresponding author at: Department of Environmental Engineering, Graduate School of Engineering, and Department of Global Ecology, Graduate School of Global Environmental Studies, Kyoto University, Kyoto-Daigaku-Katsura, Nishikyo-ku, Kyoto 615-8540, Japan.

E-mail address: fujiwara.taku.3v@kyoto-u.ac.jp (T. Fujiwara).

<https://doi.org/10.1016/j.jwpe.2025.107065>

Received 20 November 2024; Received in revised form 14 January 2025; Accepted 19 January 2025

Available online 25 January 2025

2214-7144/© 2025 The Authors. Published by Elsevier Ltd. This is an open access article under the CC BY-NC-ND license (<http://creativecommons.org/licenses/by-nc-nd/4.0/>).

concentration efficiency is an ancillary effect of a higher flux, as a larger volume of water permeates the DS, while most solutes remain on the FS side. However, the higher flux also promotes the movement of solutes and particles toward the membrane, potentially exacerbating fouling due to their accumulation on the membrane.

Our recent review [8], based on experimental data from previous studies, confirmed key trends regarding the effects of temperature on FO membrane performance and intrinsic membrane parameters. Notably, most studies on synthetic and real municipal wastewater filtration, whether using stand-alone or hybrid FO membrane systems, indicate that elevated temperatures increase flux and RSF. Moreover, higher temperatures have been associated with lower rejection efficiencies [9,10] and an increase in membrane fouling, reflected by greater solute accumulation in fouling layers or declining flux during filtration [9,11–13]. However, contradictory findings have been reported. For example, Wang et al. [14] and Zheng et al. [15] observed a decline in permeate flux, which they attributed to a lower osmotic potential. Wang et al. [14] rationalized this reduction in terms of the decomposition of ammonium bicarbonate, which was used as the DS, at temperatures above 30 °C. Meanwhile, Zheng et al. [15] linked this decline to a significant increase in the RSF at higher temperatures, which led to a sharp increase in solute concentration in the FS and a decrease in the osmotic pressure gradient. In contrast, Jeong et al. [16] suggested that the lower RSF at higher temperatures was due to hindrance caused by the enhanced permeate flux, which limited solute diffusion from the DS and minimized the formation of scalants through interactions between solutes in the DS and FS, thereby reducing membrane scaling.

Although FO membrane systems have demonstrated potential for concentrating municipal wastewater, reducing the load and potentially increasing solute concentrations to levels suitable for subsequent treatments like anaerobic digestion, their performance is significantly influenced by temperature, with previous studies revealing conflicting results on its effects under varying conditions. Additionally, the absence of reported solute concentration factors in real wastewater filtration scenarios is a notable gap identified in the literature which hinders assessing concentration efficiency in the FO process. Furthermore, the relationship between temperature and membrane fouling during sewage filtration, which has predominantly been observed through flux decline rates in existing studies, requires deeper evaluation to provide a more comprehensive understanding. The lack of investigations into potential degradation on the FS side attributable to microbial activity or oxidation, despite its potentially significant impact on solute concentration within the FS, is of particular concern. Consequently, further research is needed to elucidate the effects of temperature on concentrating municipal wastewater using FO.

This study aimed to evaluate the filtration and concentration efficiency of the FO membrane process and investigate membrane fouling behavior under various temperature conditions. Real low-strength sewage served as the FS for fouling, whereas pure water and laboratory-prepared NaCl solutions were used as the baseline FS for comparative analysis. The laboratory-scale experiments involved filtration runs with sewage under both anaerobic and non-anaerobic conditions to discern the impact of biodegradation on filtration efficiency and the composition of the fouling layer.

2. Materials and methods

2.1. Materials and equipment

FTS H₂O™ flat-sheet cellulose triacetate membranes (Sterlitech Corp., USA) were used in this study. Membrane sheets were cut into uniformly sized coupons, rinsed multiple times, soaked in ultrapure water overnight, and rinsed again to remove any packaging chemicals before use. Membrane coupons were fitted into CF042A acrylic crossflow-type membrane cells (Sterlitech), each with an active membrane area of 42 cm² and a channel depth and width of 0.23 and 3.9 cm,

respectively. Solution containers, pumps, and membrane cells were connected with polytetrafluoroethylene tubes to limit inner-wall stain when real solutions were used. Self-made pulsation dampeners were placed inline after the pumps to regulate stable flow into the membrane cell. The FO membrane system setup is shown in Fig. 1.

Ultrapure water with a resistivity of 18.2 MΩ•cm from a Barnstead™ MicroPure™ water purification system (Thermo Fisher Scientific Inc., USA) was used as the FS during pure water filtration, for reagent preparation, and for cleaning purposes. Effluent from primary sedimentation tanks in a sewage treatment plant in a city in Japan was used as the FS in sewage filtration experiments, which was stored at 4 °C within 1 h of collection. The sewage was thoroughly mixed and allowed to settle for approximately 30 min before any experiment. The supernatant was then transferred directly into the FS containers for FO experiments without additional pre-filtration. This supernatant had a pH of 6.93–6.95, electrical conductivity (EC) of 59.5–59.6 mS/m, chemical oxygen demand (COD) of 129–163 mg/L, total nitrogen (TN) of 19.0–19.3 mg/L, and total phosphorus (TP) of 2.13–2.24 mg/L; additional parameters are provided in Supplementary Information's Table S3. The DS was prepared using sodium chloride (NaCl, ≥99.5 % mass/mass, Fujifilm Wako Pure Chemical Corp., Japan).

The DS and FS were mixed continuously with magnetic stirrers (Advantec Group, Japan; IKA Works GmbH & Co. KG., Germany) to produce a homogeneous state throughout filtration. The DS and FS were recirculated between the containers and membrane cells using peristaltic pumps (Tokyo Rikakikai Co. Ltd., Japan). Dosing pumps (As One Co. Ltd., Japan) provided saturated NaCl solution to the DS to maintain a set EC throughout the filtration process. The dosing systems were regulated according to the real-time EC values of the DS and managed by an EC controller system from Climatec, Inc. (Japan) using a CR300 data logger and PC200W software from Campbell Scientific Inc. (USA). The weights of the DS and FS were measured using electronic balances from Shinko Denshi Co. Ltd. (Japan), while the weights of the saturated NaCl solutions were determined using electronic balances from A&D Co. Ltd. (Japan). The corresponding software, the RTS Input Tool (Shinko Denshi) and RsWeight (A&D), recorded data every minute.

2.2. Experiments

The two FO membrane systems were operated simultaneously under the same experimental conditions with each setup functioning independently and providing two replicates for each set of conditions. The FO filtration run included three stages: pure water filtration for 1 h, sewage filtration for 24 h to facilitate the fouling formation, and a final 1-h of pure water filtration through the fouled membrane. The system stabilization time for each stage was approximately 5 min. A three-stage filtration run was conducted using the same membrane coupons, with new coupons replacing the old ones for each subsequent filtration under different conditions. The membrane was positioned in the membrane cell with the active layer facing the FS side and the support layer facing the DS side (AL-FS mode) which has been reported to facilitate less membrane fouling [1,17,18]. A plastic mesh spacer was placed on the DS side of the flow channel to reduce external concentration polarization and improve flow turbulence.

A 1.2 M NaCl solution was used as the DS; its concentration was maintained throughout the filtration process and was renewed before each stage. Ultrapure water and real sewage were used as the FS during 1-h pure water filtration and 24-h fouling formation, respectively. The DS and FS were pumped into the membrane cell in co-current mode at a crossflow velocity of 8.5 cm s⁻¹ (flow rate of approximately 398 mL•min⁻¹). The system and solution temperatures were maintained by an incubator at 10, 20, or 30 °C (±1 °C). An up-to-2 °C temperature difference was observed during the first 10–15 min of filtration, with negligible impact on final performance as confirmed by pre-experiment stabilization tests. During sewage filtration, the FS side was sealed to prevent exterior air from penetrating. Gas bags were connected to the FS

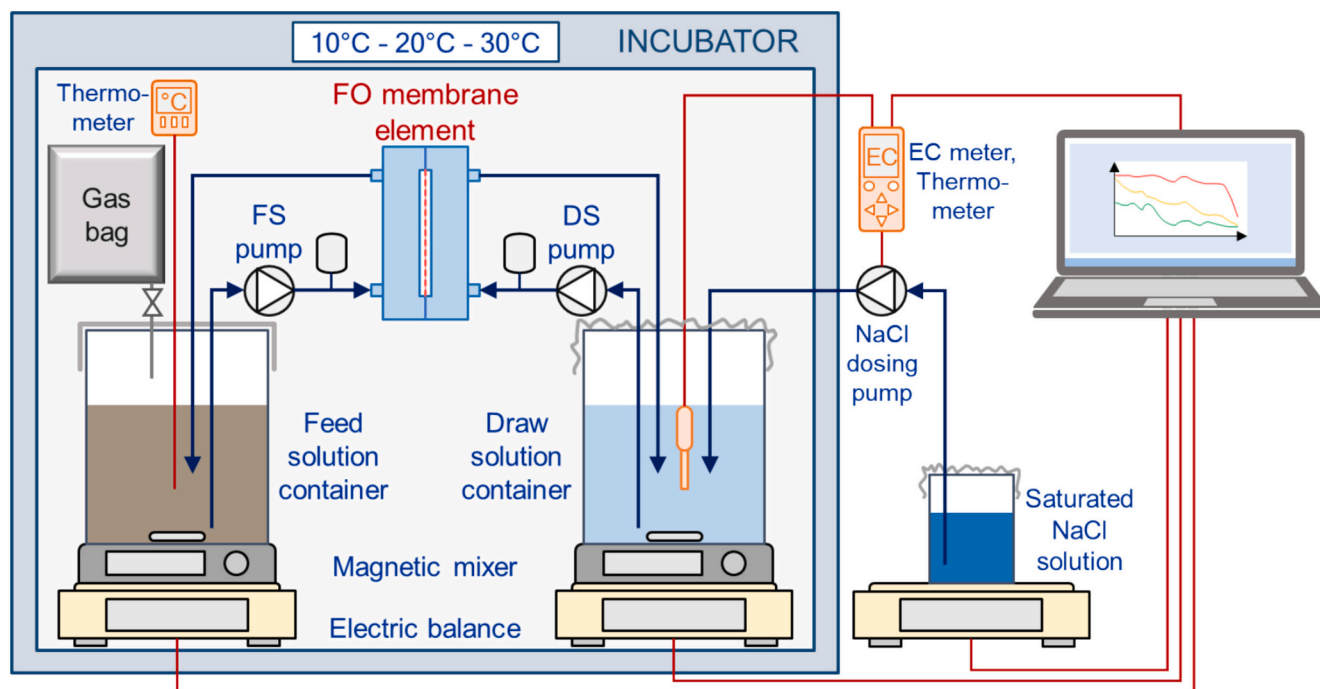


Fig. 1. FO membrane system setup.

containers to offset the volume reduction due to water permeation through the membrane. Two conditions were tested. Under anaerobic conditions (denoted as $A_{xx}^{\circ}C$, where 'xx' represents the temperature), sewage was pre-aerated with nitrogen gas to reduce its dissolved oxygen (DO) concentration to $<0.3 \text{ mg}\cdot\text{L}^{-1}$, the gas bag was filled with 1.5 L of N_2 gas, and all channels on the FS side were filled with N_2 . Under non-anaerobic conditions ($N_{xx}^{\circ}C$), sewage with a DO of $>1.0 \text{ mg}\cdot\text{L}^{-1}$ was used in its original state, gas bags were filled with normal air, and the FS side was sealed.

DS and FS samples were collected before and after sewage filtration. The FS during pure water filtration was also sampled to examine any residual solutes on the FS side, including membrane cells and tubes. The fouled membrane coupons were cut in half, and one half of each membrane was immersed in 50 mL of ultrapure water and ultrasonicated at 20 kHz for 2 min using a VC-750 Ultrasonic Liquid Processor (Sonics & Materials Inc., USA) equipped with a converter and probe to detach the fouling layer from the membrane and create a uniform suspension. The other half of each membrane was stored at $-20^{\circ}C$ for further analysis. Permeate flux was calculated from changes in weights, volumes, and densities of the DS, FS, and saturated NaCl solutions.

For comparison, baseline 24-h filtration experiments using ultrapure water ($W_{xx}^{\circ}C$) or 20 mM NaCl solution ($B_{xx}^{\circ}C$) as the FS were conducted at 10, 20, and $30^{\circ}C$ ($\pm 1^{\circ}C$). The selected NaCl solution concentration of 20 mM was within the typical range of 10 to 40 mM, commonly used to simulate background ionic strength or electrolytes in wastewater. Values of the intrinsic parameters of the membrane, including its water and solute permeability coefficients, were determined as described in Note S1 and used to calculate theoretical fluxes ($T_{xx}^{\circ}C$). The kinetic studies described in Note S2 were used to determine the degradation rate constants of the solutes in real sewage.

2.3. Analysis and calculations

EC was measured using a portable EC meter (DKK-TOA Corp., Japan), pH was measured using a portable pH meter (Horiba Advanced Techno Co. Ltd., Japan), and temperature was determined using a thermos recorder (T&D Corp., Japan), an integrated thermo-sensor in incubators, or a portable meter. COD was analyzed by the dichromate

method using COD digestion vials (Cat. 2125815 for the $3\text{--}150 \text{ mg}\cdot\text{L}^{-1}$ range, and Cat. 2125915 for the $20\text{--}1500 \text{ mg}\cdot\text{L}^{-1}$ range) and DR1900 portable spectrophotometers (HACH Co., USA). Total organic carbon (TOC) was measured using a Sievers TOC analyzer (GE Water & Process Technologies, USA). The five-day biochemical oxygen demand (BOD_5), TN, ammonia nitrogen (N-NH_4^+), TP, and orthophosphate (P-PO_4^{3-}) were analyzed following methods 5210B, 4500-N C, 4500-NH₃ G, 4500-P H, and 4500-P F, respectively, as presented in Standard Methods for the Examination of Water and Wastewater [19]. Na^+ concentrations were determined using a Dionex ICS-1100 ion chromatograph (Thermo Fisher Scientific). Excitation-emission matrix (EEM) analysis was performed using an RF-5300PC Spectrofluorophotometer (Shimadzu Corp., Japan) with the excitation and emission wavelengths of 220–420 nm and 220–550 nm, respectively, and a wavelength interval of 5 nm.

Forward permeate flux and RSF were calculated as follows:

$$J_W = \frac{\Delta V}{A_M \Delta t} = \frac{\Delta m}{\bar{\rho} A_M \Delta t}, \quad (1)$$

where J_W ($\text{L}\cdot\text{m}^{-2}\cdot\text{h}^{-1}$, or LMH) is the forward permeate flux of water, ΔV (L) and Δm (g) are changes in the volume and weight of the FS within the filtration time Δt (h), respectively (as detailed in Section 2.2), A_M (m^2) is the effective area of the membrane, and $\bar{\rho}$ ($\text{g}\cdot\text{L}^{-1}$) is the average FS density before and after filtration.

$$J_S = \frac{\Delta n_{\text{Na}^+}}{A_M \Delta t}, \quad (2)$$

where J_S ($\text{mol}\cdot\text{m}^{-2}\cdot\text{h}^{-1}$, or molMH) is the reverse solute flux, and Δn_{Na^+} (mol) is the change in the amount of Na^+ ions in the FS, as determined from the Na^+ molar concentrations in the FS before and after filtration.

The theoretical permeate flux and RSF were calculated using the obtained membrane permeability coefficients (Fig. S1), solution-diffusion model [6,7], and Fick's law [20]. Theoretical fluxes were calculated under ideal conditions, assuming the solution was perfectly mixed and had uniform solute concentrations throughout the bulk liquid, thereby eliminating concentration polarization at the membrane-solution interfaces:

$$J_{W,T} = A\sigma(\pi_{D,b} - \pi_{F,b}), \quad (3)$$

$$J_{S,T} = B(C_{D,b} - C_{F,b}), \quad (4)$$

where $J_{W,T}$ (LMH) and $J_{S,T}$ (molMH) are the theoretical permeate flux and RSF, respectively, A (LMH \cdot bar $^{-1}$) and B (LMH) are the water and solute permeability coefficients of the membrane, respectively, σ ($= 1$) is the osmotic reflection coefficient, $\pi_{D,b}$, and $\pi_{F,b}$ (bar) are the bulk liquid osmotic pressures of the DS and FS, respectively, and $C_{D,b}$ and $C_{F,b}$ (M) are the molar concentrations of Na $^{+}$ in the DS and FS, respectively. Osmotic pressure was calculated using van't Hoff equation [5]:

$$\pi = iCRT, \quad (5)$$

where π (bar) is the osmotic pressure, i is the van't Hoff factor ($i = 2$ for NaCl assuming 100 % dissociation), C (M) is the molar concentration, R (≈ 0.083 L \cdot bar \cdot K $^{-1}$ \cdot mol $^{-1}$) is the ideal gas constant, and T (K) is the absolute temperature. In these calculations, the molar concentrations of NaCl (or Na $^{+}$) in the DS and FS were fixed at 1.2 M and 20 mM, respectively, which corresponded to the concentrations of DS and FS used in the baseline filtration experiment.

Volume reduction and solute concentration factors, and solute rejection efficiencies were calculated as follows:

$$RF = \frac{V_{F,0}}{V_F}, \quad (6)$$

$$CF = \frac{C_F}{C_{F,0}}, \quad (7)$$

$$RE = \left(1 - \frac{m_{\text{Permeate}}}{m_{F,0}}\right) \times 100\%, \quad (8)$$

where RF is volume reduction factor, CF is solute concentration factor, RE (%) is solute rejection efficiency, $V_{F,0}$ and V_F (L) are the initial and final FS volumes, respectively, $C_{F,0}$ and C_F (mg \cdot L $^{-1}$) are the initial and final solute concentrations in the FS, respectively, $m_{F,0}$ (mg) is the initial solute mass in the FS, and m_{Permeate} (mg) is the solute mass permeating

from the FS to the DS, as determined by analyzing the DS after filtration.

The mass balance of the FS solutes is expressed using the following equations:

$$m_{F,0} = m_F + m_{\text{Permeate}} + m_{\text{Fouling}} + m_{\text{Degradation}}, \quad (9)$$

where m_F (mg) is the final solute mass in the FS, m_{Fouling} (mg) is the solute mass in the fouling layers on the membranes (and experimental apparatus), and $m_{\text{Degradation}}$ (mg) is the mass of solutes degraded, calculated using the equations provided in Note S2. Additional details on the mass balance are provided in Note S3.

3. Results and discussion

3.1. Effect of temperature on permeate flux

This section presents an investigation into the effects of temperature on the forward permeate flux and RSF. As depicted in Fig. 2(a), higher permeate fluxes were recorded at higher temperatures, while the RSF generally exhibited an upward trend. Specifically, the permeate fluxes of ultrapure water and 20 mM NaCl solution increased by 77.3 % and 78.5 %, respectively, when the temperature was increased by 20 $^{\circ}$ C, reaching 11.7 and 11.1 LMH at 30 $^{\circ}$ C. The permeate flux during sewage filtration grew by 61.4–66.0 %, peaking at 10.6 LMH at 30 $^{\circ}$ C under anaerobic conditions. Except for the non-anaerobically filtered sewage, the RSFs increased by $(1.50\text{--}2.95) \times 10^{-2}$ molMH with a 20 $^{\circ}$ C increase in temperature during the measurement experiments. Meanwhile, the theoretical permeate flux and RSF increased by 103 % (from 17.0 to 34.6 LMH) and 80 % (from 18.4 to 33.3×10^{-2} molMH), respectively, within the same temperature range. According to van't Hoff equation, the osmotic pressure of a solution is directly proportional to temperature, suggesting that higher temperatures enhance the driving force for the FO process. Additionally, other hydrodynamic parameters, such as solubility, viscosity, and diffusivity, increase with temperature, which is believed to improve mass transfer and thin the membrane-solution boundary layers, thereby enhancing both permeate flux and RSF. These findings are consistent with previous studies on synthetic and real

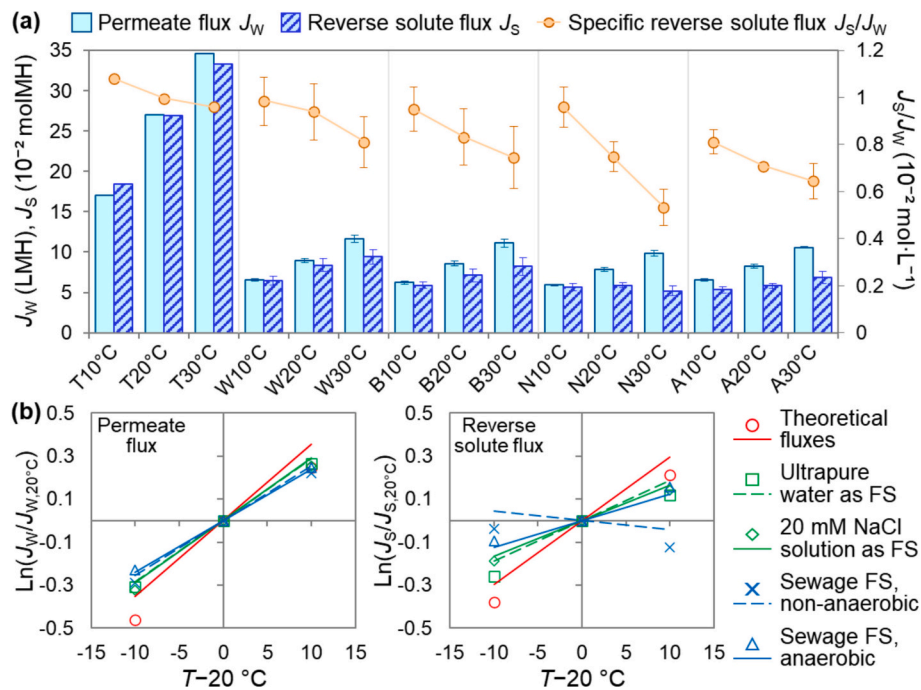


Fig. 2. (a) Theoretical and measured permeate and reverse solute fluxes across varying FSs and at various temperatures. (b) Fluxes at various temperatures referenced against those at 20 $^{\circ}$ C (room temperature). Symbols: T, theoretical fluxes; W, ultrapure water as FS; B, baseline 20 mM NaCl as FS; N, sewage FS under non-anaerobic conditions; A, sewage FS under anaerobic conditions. Error bars represent standard deviations determined from two replicates.

municipal wastewater, which reported that higher temperatures lead to increased permeate fluxes and RSFs [8]. Table S4 provides a comparison between the findings of the current study and those reported in previous works.

Theoretical fluxes were found to increase notably with increasing temperature. With constant DS and FS concentrations set for the calculations, the osmotic pressure difference between the two solutions increased by approximately 7 % as the temperature rose from 10 °C (283.15 K) to 30 °C (303.15 K). Hence, the significant enhancement in the theoretical flux is attributable to substantial changes in the permeability coefficients of both water and the solutes across the membrane (Fig. S1). These increases in water and solute permeability coefficients with increasing temperature are consistent with findings from previous studies [21–24]. Membrane parameters were calculated from the experimental results; consequently, their increases are possibly attributable to enhanced mass transfer at elevated temperatures. Alternatively, physical dilation of the membrane, which results in pore expansion and facilitating water and solute permeation, is another possible reason. However, advanced techniques are required to directly measure and confirm this notion.

While the flux increases occurred similarly, the rates of change determined for the theoretical and actual filtrations were different. Fig. 2(b) illustrates that the theoretical flux exhibits the most pronounced increase with temperature, followed by the pure water and NaCl solution filtration fluxes, and finally the real sewage filtration fluxes. These changes were quantified by calculating the temperature coefficient (θ) using the equation: $J_T/J_{20^\circ\text{C}} = \theta^{(T-20^\circ\text{C})}$, which is based on the van't Hoff–Arrhenius relationship [25], the results of which are listed in Table S5. The θ value of the permeate flux ranged from 1.024 to 1.036, with the theoretical flux exhibiting the highest value and the sewage filtration flux the lowest. The RSFs also exhibited comparable trends.

Several factors contribute to the differences mentioned above. Firstly, theoretical calculations assume ideal conditions with completely mixed solutions, uniform concentrations throughout the bulk liquid and membrane surfaces, and unidirectional permeate flow, where water permeates from the FS to the DS and solute diffuses from the DS to the FS. However, concentration polarization (CP) occurs under practical conditions, which reduces the osmotic gradient across the membrane and the driving force for permeation, thereby significantly decreasing the flux. The behavior of CP in response to temperature remains inconclusive; while some studies suggest that it is alleviated at higher temperatures, others suggest that its severity increases (evidenced by a decrease in the ratio of the effective osmotic pressure difference to the theoretical one) [8]. However, the adverse effects of CP on flux behavior are obvious; hence, they may also lower the rate of flux change.

Secondly, while the theoretical permeate flux and RSF are assessed individually, in practice, they occur simultaneously, leading to a reduction in the FS volume and an increase in the solute concentration. The FS becomes more concentrated at elevated temperatures owing to the increased concentration of solutes initially present in the solution (e.g., organics and nutrients, as indicated by changes in their concentration factors; see Section 3.2) and solutes diffusing from the DS (i.e., NaCl, as evidenced by the higher RSF). The rise in FS concentration increased the osmotic pressure on the FS side, thereby reducing the osmotic gradient across the membrane compared to theoretical expectations, which caused the actual flux to increase at a slower rate. Nevertheless, the concurrency of permeate and reverse solute fluxes offers several benefits. As shown in Fig. 2(a), the specific reverse solute flux decreases more significantly during actual filtration than theoretically calculated, which suggests that the higher permeate flux at elevated temperatures may predominate and restrain the solute flux from the DS. Heo et al. [26] attributed this behavior to a greater increase in water flux at higher temperatures, owing to improved membrane wettability, higher solute diffusivity back to the DS (which reduces the RSF), and structural changes in the membrane that favor water molecule diffusion over

solute diffusion.

The rate of flux change with temperature is also influenced by membrane fouling. The formation of fouling layers obstructs water permeation, resulting in a gradual decrease in permeate flux (Fig. 3) and a lower overall flux. Consequently, although the flux from the sewage FS still increased with increasing temperature, the membrane fouling layers moderated the magnitude of this rise compared with both the baseline and theoretical fluxes, as evidenced by the trend lines in Fig. 2(b). However, membrane fouling layers can also impede the solute diffusion from the DS, which is indicated by a slower increase in the RSF or even a decrease at higher temperatures in the case of non-anaerobic sewage filtration, leading to an accelerated decline in the specific reverse solute flux (Fig. 2(a)). These observations underscore the benefits of a higher solution temperature, as it augments the permeate flux and enhances water recovery, while the concentrated FS following filtration is less saline and suitable for use as a feed in other processes, such as anaerobic digestion.

Relationships between membrane fouling and permeate flux at various temperatures are shown in Fig. 3, which displays the normalized flux profile against cumulative permeate volume for visual comparison. Flux remained relatively stable in the absence of membrane fouling throughout pure water and NaCl solution filtrations and only decreased slightly owing to reverse solute diffusion, which increased the FS concentration and reduced the osmotic gradient across the membrane. Conversely, sewage filtration led to the accumulation of particles from the FS on the membrane that formed fouling layers. Interestingly, despite the higher water permeation at elevated temperatures, which potentially brings more particles that form fouling layers, the decline in flux after 24 h of filtration was consistent across the three operating temperatures and ranged between 30 % and 40 % of the initial flux. This observation indicates that flux declined more slowly at higher temperatures when an equivalent volume of water permeated the membrane. Kim et al. [27] and Xiao et al. [28] have suggested that particles simultaneously attach to and detach from the membrane, implying that membrane fouling progresses more gradually at higher temperatures. The slower fouling development can extend the filtration process before membrane cleaning becomes necessary, representing an additional benefit of FO membrane filtration at elevated temperatures, along with higher permeate flux and increased water recovery.

3.2. Effect of temperature on filtration performance

Evaluating the performance of a sewage treatment process necessitates determining the solute rejection efficiency. In this study, the rejection efficiencies of organics (TOC, COD), nitrogen (TN, NH_4^+), and phosphorus (TP, PO_4^{3-}) during FO filtration at various temperatures were assessed, with the results shown in Fig. 4(a). Phosphorus was remarkably retained on the FS side, with a rejection rate approaching 100 % at all examined temperatures, while the rejection efficiency of organic matter declined only marginally (by <1 %) as the temperature was increased from 10 to 30 °C. Conversely, nitrogen permeation into the DS increased significantly with increasing temperature, leading to a notable decrease in the rejection rate. Both TN and NH_4^+ rejection dropped from 95.9 % to 88.1 % under non-anaerobic conditions, whereas the decline was more pronounced, from 95 % to 82.1 %, under anaerobic conditions. This difference is ascribable to the smaller ionic size of ammonia nitrogen compared to those of phosphate and organic compounds; hence it passes through the membrane more easily. This hypothesis is supported by several studies in which membrane traversability was compared based on molecular size [29–32]. Furthermore, thermal dilation of membrane pores facilitates solute traversal, leading to higher permeation and lower rejection efficiency of small molecules at elevated temperatures.

Bidirectional diffusion has been suggested to affect the nitrogen rejection efficiency. Previous studies observed the bidirectional diffusion of Na^+ and NH_4^+ between the DS and FS [9,33–35]. Notably, NH_4^+

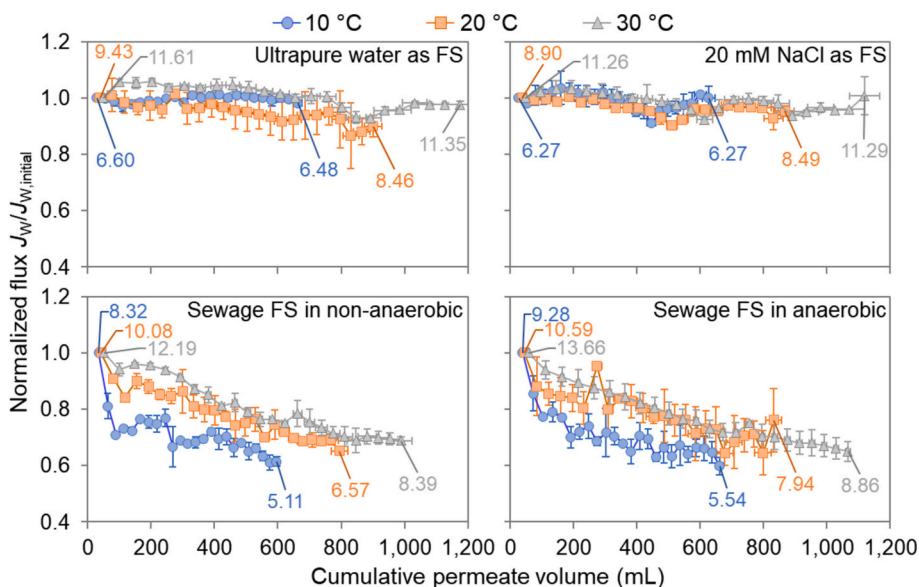


Fig. 3. Permeate flux normalized against the initial flux (first hour) across varying FSs and temperatures. Data labels indicate the initial and final fluxes (at 24 h, when filtration was completed). Error bars represent standard deviations determined from two replicates.

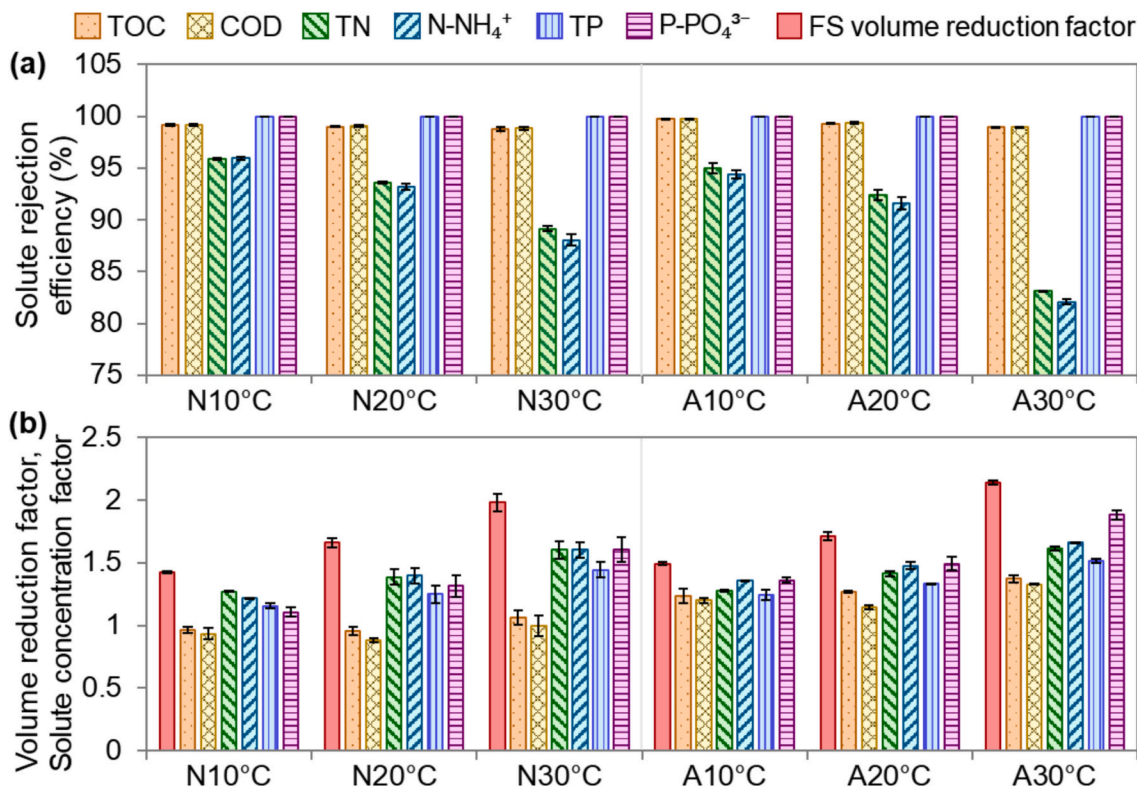


Fig. 4. (a) Solute rejection efficiencies after sewage filtration for 24 h. (b) Solute concentration factors relative to FS volume reduction factors after sewage filtration for 24 h. N: non-anaerobic sewage; A: anaerobic sewage. Error bars represent standard deviations determined from two replicates.

permeation from the FS was more pronounced when a strong electrolyte, such as NaCl, was used as the DS, compared to nondissociated or large hydration ion-forming dissociated DSs [33]. In this study, higher Na⁺ diffusion from the NaCl DS, combined with membrane pore expansion at elevated temperatures, likely intensified NH₄⁺ permeation from the FS to the DS, leading to lower ammonia nitrogen rejection. Bidirectional H⁺ and Na⁺ diffusion between the two solutions has also been previously proposed, with the reverse diffusion of Na⁺ from the DS potentially

driving H⁺ away from the FS, leading to a rise in the pH of the FS [34,36]. The loss of H⁺ from the FS, along with changes in solution salinity due to solute concentration and reverse solute diffusion, is possibly responsible for the observed increases in FS pH (by 0.04–0.71 units) from its initial value of 6.94 ± 0.04, with more pronounced increases observed at higher temperatures. Additionally, the ammonia dissociation constant (pKa) was observed to decrease from 9.73 to 9.09 as the temperature was increased from 10 to 30 °C, consistent with a

relationship reported in the literature [37], from which the equation was used for calculation. These shifts in pKa and pH at elevated temperatures shift the ammonia equilibrium from NH_4^+ toward NH_3 , with the latter diffusing more readily through the membrane, thereby lowering NH_4^+ rejection. The literature also confirms the effects of higher temperatures and pH levels on the ammonia equilibrium [38,39].

One of the objectives of the FO membrane system in this study was to concentrate sewage; therefore, solute concentration efficiency was evaluated and compared with the degree of FS volume reduction. In an ideal FO system, only water should permeate the membrane, while all solutes are retained, leading to solute concentration factors that match the reduction in FS volume. However, as shown in Fig. 4(b), although the solute concentration factors trended upward with increasing temperature, they remained low compared with the degrees of volume reduction at the same operating temperatures. While FS volume was reduced by factors of 1.42–1.98 under non-anaerobic conditions and 1.49–2.14 under anaerobic conditions, the nitrogen concentration increased by factors of only 1.21–1.66 as the temperature was increased from 10 to 30 °C, with consistent behavior observed under both sets of conditions. On the other hand, the phosphorus concentration factor rose from 1.11 to 1.60 during non-anaerobic filtration and from 1.24 to 1.88 during anaerobic filtration in the same temperature range. Conversely, the TOC and COD concentration factors fluctuated around 1.0 under non-anaerobic conditions, with higher values of 1.20–1.37 recorded under anaerobic conditions. The observed post-filtration increases in concentration factors are attributable to rapid FS volume reduction owing to higher permeate fluxes at elevated temperatures. This phenomenon has also been observed previously when FO was used to concentrate various substances, such as glucose and sucrose [40], pasteurized milk [41], anthocyanin [42], and geothermal brine [43].

The discrepancies between solute concentration factors and volume reduction factors, particularly at higher temperatures (20 and 30 °C), and more significantly for organic matter, raise concerns about concentration efficiency at elevated temperatures. Several factors may have contributed to this low concentration efficiency. First, solutes may permeate the DS along with the water flux, which is particularly evident for nitrogen, where the rejection efficiency decreases with increasing temperature (Fig. 4(a)). Meanwhile, the high rejection rates of organics and phosphorus suggest possible losses on the FS side. Analysis of the fouled membranes (detailed in Section 3.3) revealed the presence of residual organics and nutrients in the fouling layers. Additionally, solutes were also found to adhere to the experimental apparatus (tubes and membrane cells). Biodegradation, which is more pronounced for organic matter, provides another potential reason for solute loss in the FS. Organics are more intensely oxidized under non-anaerobic conditions than anaerobic conditions owing to the presence of oxygen. Kinetic studies have also revealed higher reaction rates at higher temperatures. As a result, organics exhibited lower and less variable concentration factors than the nutrient and FS volume reduction factors. Mass balances were evaluated for further insight, with details provided in Section 3.4.

3.3. Effects of temperature on the composition of the membrane fouling layer

Fouled membranes were analyzed to investigate the impact of temperature on membrane fouling. Fig. 5(a) reveals that the quantity of solutes within the fouling layer increased with increasing operating temperatures in the anaerobic experiment. Specifically, notable increases in accumulated organic matter, including TOC, COD, and BOD_5 , by 22.9–61.7 % were recorded as the operating temperature was increased by 20 °C. Interestingly, more TN and TP mass accumulated on the membrane when the temperature was increased from 10 to 20 °C compared with that recorded for the 20 to 30 °C increase. Conversely, the amounts of organics and nutrients within the membrane fouling layers increased as the temperature was increased from 10 to 20 °C during non-anaerobic filtration; however, they declined as the

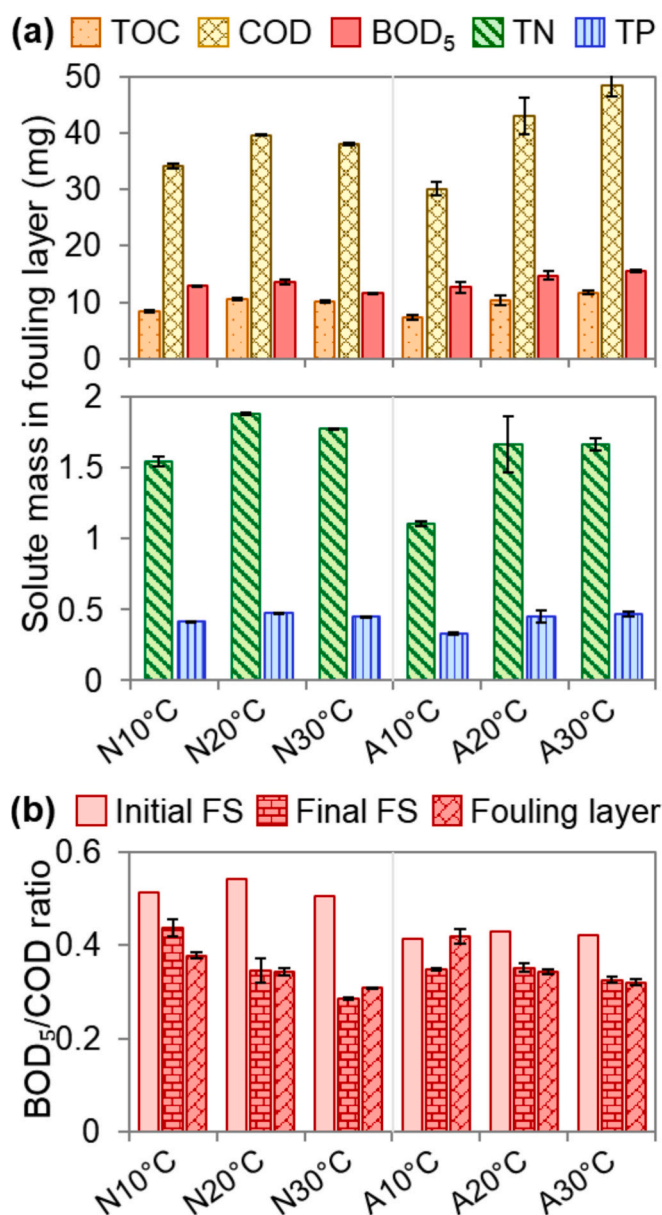


Fig. 5. (a) Solute mass accumulated in membrane fouling layers. (b) BOD_5/COD ratios in FSs before and after filtration, and in membrane fouling layers. N: non-anaerobic sewage; A: anaerobic sewage. Error bars represent standard deviations determined from two replicates.

temperature was further increased to 30 °C.

The increase in solute mass within the fouling layer is attributable to the heightened permeate flux, which promotes particle convection toward the membrane and contributes to fouling layer formation. However, solute buildup at the membrane surface can create a concentration gradient between the membrane-liquid interface and the bulk liquid, leading to the back diffusion of solutes from the membrane fouling layers. Some researchers have suggested that both types of solute behavior—convection toward the membrane and diffusion from the membrane—occur concurrently and may be enhanced by elevated temperatures, which indicates that fouling layer formation depends on the dominant process [27,28]. The promoted solute diffusion from the membrane fouling layers may rationalize the gradual increase or decrease in solute mass at higher temperatures observed in this study.

Reverse permeate flux is also capable of detaching particles from the fouling layer into the bulk liquid; it may result from fluid convection through the membrane facilitated by pore expansion at elevated

temperatures. Additionally, localized changes in solute concentration at the membrane-solution interfaces may play significant roles. Concentrations at the membrane-FS interface increase due to solute buildup via solute convection (from the FS), reverse solute diffusion (from the DS), and solute accumulation on the fouling layer. In contrast, concentrations at the membrane-DS interface decrease due to dilution by the permeate (the CP phenomenon). These concentration changes are more pronounced at elevated temperatures, owing to significantly enhanced permeate and reverse solute fluxes. As a result, transient conditions may arise where the solute concentration on the FS side exceeds that on the DS side, potentially triggering osmotic-driven reverse permeate flow from the DS to the FS and causing particle detachment from the fouling layer. However, reverse permeate fluxes remain hypothetical and unconfirmed, with further research needed.

The introduction of microorganisms by using real sewage as the FS in this study is another concern, as microorganisms play pivotal roles in the biodegradation of organic compounds. As shown in Fig. 5(b), the BOD₅/COD ratios demonstrate a declining trend with increasing temperature, with a more gradual decrease observed within the fouling layer. This observation indicates that the microbial proliferation during the 24-h filtration significantly altered the compositions of the FS and fouling layers, likely affecting solute distribution on the FS side and reducing solute accumulation within the fouling layers. Consequently, at an appropriately high temperature, biodegradation, coupled with the previously discussed solute back diffusion, is anticipated to limit the formation of membrane fouling layers, thereby potentially prolonging operation and reducing cleaning frequency. However, extended filtration and solute retention time may also lead to undesirable biofouling, necessitating further investigations.

The EEM plots displayed in Fig. 6 illustrate the characteristics of both the concentrated FS and the membrane fouling layer. The locations of the five regions in the EEM plots are shown in Fig. S3. A close examination reveals that the concentrations of aromatic proteins (regions I and II) and soluble microbial by-product-like compounds (region IV) in the concentrated post-filtered FS exhibited no significant changes with increasing temperature under non-anaerobic conditions; however, slight

increases were observed under anaerobic conditions. In contrast, the final FS exhibited a notable increase in fulvic acid-like (region III) and humic acid-like (region V) compounds at higher temperatures, indicating efficient concentration of compounds that are more resistant to microbial degradation. On the other hand, the membrane fouling layers exhibited different behavior. Negligible proportions of fulvic acid- and humic acid-like compounds were recorded, while the concentrations of aromatic proteins and soluble microbial by-product-like compounds varied with temperature. Specifically, these concentrations increased as the temperature was increased from 10 to 20 °C and then decreased at 30 °C. These trends are consistent with the solute quantities in the fouling layers discussed earlier, reaffirming the influence of temperature on both biodegradation and fouling dynamics.

3.4. Mass balance

Fig. 7 and Table S2 compare solute masses before and after FO membrane filtration. The solute distributions appear to be based on their characteristics and filtration efficiencies. Specifically, the proportion of solutes that permeated into the DS was more pronounced for TN, accounting for 3.7–10.7 % of the initial TN in the FS during non-anaerobic filtration, and 4.9–16.9 % during anaerobic filtration. These observations are attributable to ammonia nitrogen, which constitutes the largest fraction of TN and has a small molecular size that facilitates its ability to traverse the membrane, as reflected in the previously discussed lower rejection efficiency of N-NH₄⁺. Conversely, 14.2–27.0 % of the initial organic matter (in terms of COD and TOC) and approximately 15 % of the initial TP were found in the fouling layers on the membrane and experimental apparatus post-filtration, which is attributable to the large sizes and molecular masses of these compounds, leading to precipitation or accumulation on the surfaces of membranes, tubes, and membrane cells. Here, the effect of temperature on solute proportions is explained by the higher permeate flux at elevated temperatures, which transfers a greater volume of water across the membrane, mobilizing more solutes and particles toward the membrane and leading to either their subsequent permeation or deposition, as discussed in Sections 3.2 and 3.3.

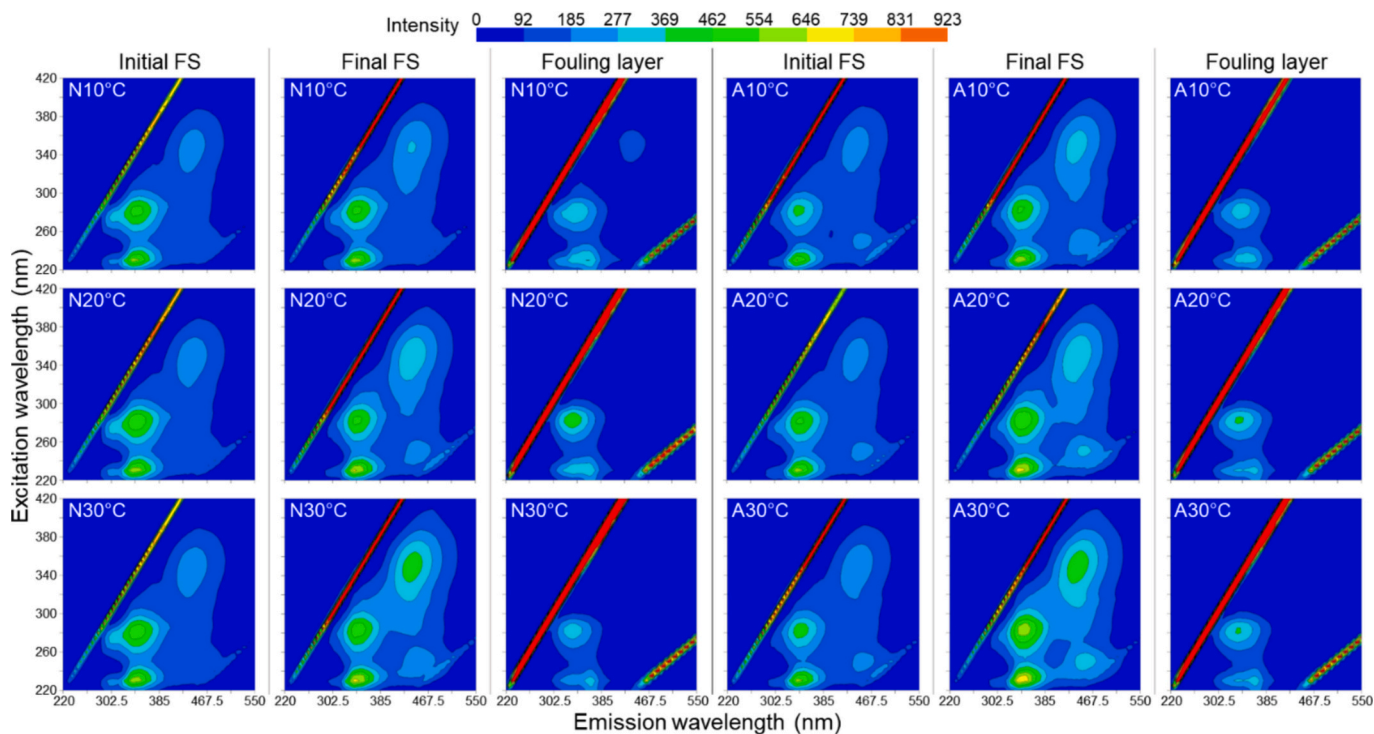


Fig. 6. EEM plots of initial and final (concentrated) FSs, and dissolved solutions of membrane fouling layers. N: non-anaerobic sewage; A: anaerobic sewage. The reader is referred to the web version for color representations.

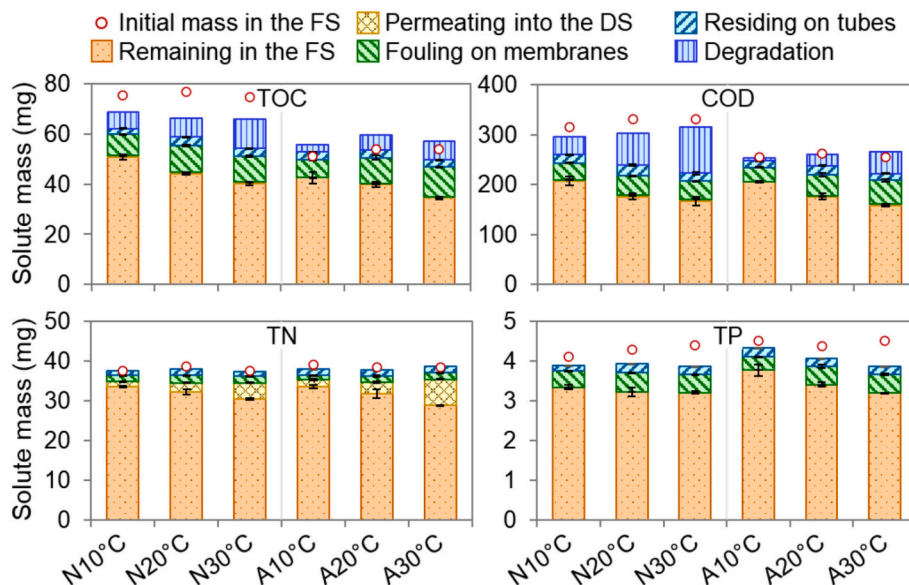


Fig. 7. Solute proportions before and after FO membrane filtration. N: non-anaerobic sewage; A: anaerobic sewage. Error bars represent standard deviations determined from two replicates.

Degraded solutes also need to be accounted for when assessing mass balance, especially when the FS contains microorganisms capable of consuming organic matter and nutrients. The mass of the degraded solute was quantified using the reaction rate constants derived from the kinetic studies detailed in Note S2. Significant organic degradation was observed, constituting up to 15.8 % and 27.7 % of the initial TOC and COD, respectively, in the FS. This proportion was higher in the non-anaerobic filtration setups, which is likely due to accelerated microbial growth in oxygen-rich environments. Meanwhile, fewer organics were lost during anaerobic conversion, as evidenced by the negligible biogas emissions determined during gas analysis (data not shown). Additionally, differences between the initial and post-filtration solute masses are possibly ascribable to differences between calculated values obtained in the independent kinetic studies and those obtained for the actual FO membrane system. The decrease in FS volume during non-anaerobic filtration may have led to oxygen dissolution and higher levels of oxidation and biodegradation. The calculations did not account for changes in the solute and microbial concentrations during filtration and only considered bulk-liquid degradation, which excluded degradation in fouling layers. These considerations highlight the opportunity to develop a more accurate model for assessing degraded solutes during FO membrane filtration.

4. Conclusions and future research perspectives

In this study, the influence of operating temperature on sewage filtration using FO membranes was thoroughly investigated. Elevating the temperature from 10 to 30 °C was found to notably increase the forward permeate flux more effectively than the RSF, resulting in a significant reduction in specific reverse solute flux. This advancement mitigates concerns associated with rapid increases in FS salinity, thereby enhancing the potential of concentrated FSs for use in additional treatment processes, such as anaerobic digestion. Despite a higher flux promoting membrane fouling and subsequent flux decline, the similar degrees of flux decline observed at all three temperatures are indicative of the delayed formation of fouling layers at higher temperatures. This observation is further supported by the slower increases, or even decreases, in the fouling layer composition at elevated temperatures, which suggests that the FO filtration system can be operated for extended operating times before membrane cleaning is required.

While only nitrogen exhibited a significant decline in rejection

efficiency with temperature, all examined parameters showed lower concentration efficiencies than anticipated and exhibited modest concentration increases with temperature. These findings raise concerns that the quality of the concentrated sewage after 24 h of filtration may not meet the influent requirements for anaerobic digestion. Mass balance assessments revealed that more solutes accumulated on the membranes and underwent biological degradation at elevated temperatures, which is the primary reason for the low concentration efficiency. Consequently, ensuring optimal filtration performance at high temperatures while minimizing material loss from fouling and degradation presents a significant challenge for future research.

Building on these findings, the method demonstrated in this study is potentially applicable to small-to-medium-scale FO membrane systems with moderate treatment volumes that use available on-site heat sources or hot waste streams. However, to fully understand the impact of temperature on membrane fouling, long-term studies are necessary. Prolonged filtration and heightened microbial activity can introduce varying fouling behavior, including biofouling, which may affect system performance. Additionally, the higher solute loss from the FS and the DS contamination due to solute diffusion at elevated temperatures necessitates careful post-filtration management and treatment strategies for these solutions. Hence, a techno-economic assessment is crucial for evaluating economic feasibility, particularly if heating the solution is required to mitigate cold-season effects and ensure stable operation of the system. Ongoing studies are focusing on systematically addressing these challenges and optimizing the process.

CRedit authorship contribution statement

Nguyen Anh-Vu: Writing – review & editing, Writing – original draft, Visualization, Methodology, Investigation, Formal analysis, Conceptualization. **Youhei Nomura:** Writing – review & editing, Validation, Supervision, Resources, Methodology, Funding acquisition. **Taira Hidaka:** Writing – review & editing, Validation, Supervision. **Taku Fujiwara:** Writing – review & editing, Validation, Supervision, Resources, Project administration, Funding acquisition.

Declaration of Generative AI and AI-assisted technologies in the writing process

The latest free version of ChatGPT (<https://chat.openai.com/>) was

used for English grammar and spelling checks, as well as for refining the expression. The authors affirm that they carefully reviewed and adjusted the content to preserve its core information after these refinements. The authors assume full responsibility for the publication's content.

Declaration of competing interest

The authors declare that they have no known competing financial interests or personal relationships that may have influenced the work reported in this study.

Acknowledgements

This study was financially supported by JST-Mirai Program Grant Number JPMJMI22I3, Japan and JSPS KAKENHI Grant Number 21K14275. The authors thank research assistants Ms. Chisumi Harada and Ms. Yoshiko Nishisaka for their support as part of this study and also acknowledge Editage (www.editage.jp) for English language editing.

Appendix A. Supplementary data

Supplementary data to this article can be found online at <https://doi.org/10.1016/j.jwpe.2025.107065>.

Data availability

Data will be made available on request.

References

- [1] S. Zhao, L. Zou, C.Y. Tang, D. Mulcahy, Recent developments in forward osmosis: opportunities and challenges, *J. Membr. Sci.* 396 (2012) 1–21, <https://doi.org/10.1016/j.memsci.2011.12.023>.
- [2] T. Cath, A. Childress, M. Elimelech, Forward osmosis: principles, applications, and recent developments, *J. Membr. Sci.* 281 (2006) 70–87, <https://doi.org/10.1016/j.memsci.2006.05.048>.
- [3] A. Haupt, A. Lerch, Forward osmosis application in manufacturing industries: a short review, *Membranes* 8 (2018) 47, <https://doi.org/10.3390/membranes8030047>.
- [4] W. Suwailah, N. Pathak, H. Shon, N. Hilal, Forward osmosis membranes and processes: a comprehensive review of research trends and future outlook, *Desalination* 485 (2020) 114455, <https://doi.org/10.1016/j.desal.2020.114455>.
- [5] G.N. Lewis, The osmotic pressure of concentrated solutions, and the laws of the perfect solution, *J. Am. Chem. Soc.* 30 (1908) 668–683, <https://doi.org/10.1021/ja01947a002>.
- [6] Z.H. Foo, D. Rehman, O.Z. Coombs, A. Deshmukh, J.H. Lienhard, Multicomponent Fickian solution-diffusion model for osmotic transport through membranes, *J. Membr. Sci.* 640 (2021) 119819, <https://doi.org/10.1016/j.memsci.2021.119819>.
- [7] J.G. Wijmans, R.W. Baker, The solution-diffusion model: a review, *J. Membr. Sci.* 107 (1995) 1–21, [https://doi.org/10.1016/0376-7388\(95\)00102-I](https://doi.org/10.1016/0376-7388(95)00102-I).
- [8] N. Anh-Vu, Y. Nomura, T. Hidaka, T. Fujiwara, Forward osmosis membrane process: a review of temperature effects on system performance and membrane parameters from experimental studies, *J. Environ. Chem. Eng.* 12 (2024) 113429, <https://doi.org/10.1016/j.jece.2024.113429>.
- [9] K. Almoalimi, Y.-Q. Liu, A. Booth, S. Heo, Temperature effects of MD on municipal wastewater treatment in an integrated forward osmosis and membrane distillation process, *Processes* 10 (2022) 355, <https://doi.org/10.3390/pr10020355>.
- [10] C. Wang, Y. Li, Y. Wang, Treatment of greywater by forward osmosis technology: role of the operating temperature, *Environ. Technol.* 40 (2019) 3434–3443, <https://doi.org/10.1080/09593330.2018.1476595>.
- [11] J. Chang, H. Qiu, J. Wang, R. Lin, B.V. Hernandez, C. Ji, et al., Efficient organic enrichment from sludge filtrate via a forward osmosis membrane process, *J. Environ. Chem. Eng.* 8 (2020) 104042, <https://doi.org/10.1016/j.jece.2020.104042>.
- [12] T. Gao, H. Zhang, X. Xu, J. Teng, M. Lu, Enhanced water and energy recovery from anaerobic osmotic membrane bioreactors treating waste activated sludge based on the draw solution concentration and temperature regulation, *Chem. Eng. J.* 417 (2021) 129325, <https://doi.org/10.1016/j.cej.2021.129325>.
- [13] S. Xia, R. Yang, X. Zhang, M. Ni, Y. Wan, L. Yao, et al., Removal of natural organic matter by forward osmosis membrane: flux behaviour and foulant characterization, *Chem. Res. Chin. Univ.* 31 (2015) 308–314, <https://doi.org/10.1007/s40242-015-4374-1>.
- [14] C. Wang, B. Gao, P. Zhao, Q. Yue, H.K. Shon, S. Yang, The forward osmosis application: using the secondary effluent as makeup water for cooling water dilution, *Desalin. Water Treat.* 105 (2018) 1–10, <https://doi.org/10.5004/dwt.2018.21983>.
- [15] L. Zheng, W.E. Price, T. He, L.D. Nghiem, Simultaneous cooling and provision of make-up water by forward osmosis for post-combustion CO₂ capture, *Desalination* 476 (2020) 114215, <https://doi.org/10.1016/j.desal.2019.114215>.
- [16] G. Jeong, D. Jang, H. Lee, A. Jang, Effects of feed solution chemistry on membrane scaling in fertilizer-drawn forward osmosis process for sustainable agricultural reuse, *Desalination* 545 (2023) 116150, <https://doi.org/10.1016/j.desal.2022.116150>.
- [17] S. Jafarnejad, Forward osmosis membrane technology for nutrient removal/recovery from wastewater: recent advances, proposed designs, and future directions, *Chemosphere* 263 (2021) 128116, <https://doi.org/10.1016/j.chemosphere.2020.128116>.
- [18] K. Lutchmiah, A.R.D. Verliefe, K. Roest, L.C. Rietveld, E.R. Cornelissen, Forward osmosis for application in wastewater treatment: a review, *Water Res.* 58 (2014) 179–197, <https://doi.org/10.1016/j.watres.2014.03.045>.
- [19] American Public Health Association (Ed.), *Standard Methods for the Examination of Water and Wastewater*, 23rd ed., APHA, Washington, DC, 2017.
- [20] M. Mulder, *Basic Principles of Membrane Technology*, Springer Netherlands, Dordrecht, 1996, <https://doi.org/10.1007/978-94-009-1766-8>.
- [21] M.R. Chowdhury, J.R. McCutcheon, Elucidating the impact of temperature gradients across membranes during forward osmosis: coupling heat and mass transfer models for better prediction of real osmotic systems, *J. Membr. Sci.* 553 (2018) 189–199, <https://doi.org/10.1016/j.memsci.2018.01.004>.
- [22] W.-J. Kim, O. Campanella, D.R. Heldman, A stepwise approach to predict the performance of forward osmosis operation: effect of temperature and flow direction, *Desalination* 538 (2022) 115889, <https://doi.org/10.1016/j.desal.2022.115889>.
- [23] J. Lee, N. Ghaffour, Predicting the performance of large-scale forward osmosis module using spatial variation model: effect of operating parameters including temperature, *Desalination* 469 (2019) 114095, <https://doi.org/10.1016/j.desal.2019.114095>.
- [24] M.C.Y. Wong, K. Martinez, G.Z. Ramon, E.M.V. Hoek, Impacts of operating conditions and solution chemistry on osmotic membrane structure and performance, *Desalination* 287 (2012) 340–349, <https://doi.org/10.1016/j.desal.2011.10.013>.
- [25] Metcalf & Eddy Inc, *Wastewater Engineering: Treatment and Resource Recovery*, 5th ed., McGraw-Hill Education, New York, 2014.
- [26] J. Heo, K.H. Chu, N. Her, J. Im, Y.-G. Park, J. Cho, et al., Organic fouling and reverse solute selectivity in forward osmosis: role of working temperature and inorganic draw solutions, *Desalination* 389 (2016) 162–170, <https://doi.org/10.1016/j.desal.2015.06.012>.
- [27] Y. Kim, S. Lee, H.K. Shon, S. Hong, Organic fouling mechanisms in forward osmosis membrane process under elevated feed and draw solution temperatures, *Desalination* 355 (2015) 169–177, <https://doi.org/10.1016/j.desal.2014.10.041>.
- [28] P. Xiao, J. Li, Y. Ren, X. Wang, A comprehensive study of factors affecting fouling behavior in forward osmosis, *Colloids Surf. A* 499 (2016) 163–172, <https://doi.org/10.1016/j.colsurfa.2016.04.014>.
- [29] N. Asghar, H. Lee, D. Jang, A. Jang, Recovery of volatile fatty acids using forward osmosis: influence of solution chemistry, temperature, and membrane orientation, *Chemosphere* 303 (2022) 134814, <https://doi.org/10.1016/j.chemosphere.2022.134814>.
- [30] M. Xie, L.D. Nghiem, W.E. Price, M. Elimelech, Relating rejection of trace organic contaminants to membrane properties in forward osmosis: measurements, modelling and implications, *Water Res.* 49 (2014) 265–274, <https://doi.org/10.1016/j.watres.2013.11.031>.
- [31] W. Xue, T. Tobino, F. Nakajima, K. Yamamoto, Seawater-driven forward osmosis for enriching nitrogen and phosphorus in treated municipal wastewater: effect of membrane properties and feed solution chemistry, *Water Res.* 69 (2015) 120–130, <https://doi.org/10.1016/j.watres.2014.11.007>.
- [32] S. Yang, B. Gao, A. Jang, H.K. Shon, Q. Yue, Municipal wastewater treatment by forward osmosis using seawater concentrate as draw solution, *Chemosphere* 237 (2019) 124485, <https://doi.org/10.1016/j.chemosphere.2019.124485>.
- [33] K. Almoalimi, Y.-Q. Liu, Enhancing ammonium rejection in forward osmosis for wastewater treatment by minimizing cation exchange, *J. Membr. Sci.* 648 (2022) 120365, <https://doi.org/10.1016/j.memsci.2022.120365>.
- [34] N.T. Hancock, T.Y. Cath, Solute coupled diffusion in osmotically driven membrane processes, *Environ. Sci. Technol.* 43 (2009) 6769–6775, <https://doi.org/10.1021/es901132x>.
- [35] X. Lu, C. Boo, J. Ma, M. Elimelech, Bidirectional diffusion of ammonium and sodium cations in forward osmosis: role of membrane active layer surface chemistry and charge, *Environ. Sci. Technol.* 48 (2014) 14369–14376, <https://doi.org/10.1021/es504162v>.
- [36] M. Xie, W.E. Price, L.D. Nghiem, Rejection of pharmaceutically active compounds by forward osmosis: role of solution pH and membrane orientation, *Sep. Purif. Technol.* 93 (2012) 107–114, <https://doi.org/10.1016/j.seppur.2012.03.030>.
- [37] Australian and New Zealand Environment and Conservation Council, *Agriculture and Resource Management Council of Australia and New Zealand, volume 2. Aquatic ecosystems — rationale and background information*, in: Australian and New Zealand Guidelines for Fresh and Marine Water Quality, ANZECC and ARMCANZ, Canberra, 2000. <https://www.waterquality.gov.au/sites/default/files/documents/anzec-armcanz-2000-guidelines-vol2.pdf>.
- [38] K. Emerson, R.C. Russo, R.E. Lund, R.V. Thurston, Aqueous ammonia equilibrium calculations: effect of pH and temperature, *J. Fish. Res. Board Can.* 32 (1975) 2379–2383, <https://doi.org/10.1139/f75-274>.
- [39] J.-C. Huang, C. Shang, Air stripping, in: L.K. Wang, Y.-T. Hung, N.K. Shammam (Eds.), *Advanced Physicochemical Treatment Processes*, Humana Press, Totowa, NJ, 2006, pp. 47–79, https://doi.org/10.1007/978-1-59745-029-4_2.

- [40] S. Xiao, Z. Li, Q. Xiong, C. Wu, J. Huang, R. Zhou, et al., Exploration of sodium lactate as the draw solute of forward osmosis for food processing, *J. Food Eng.* 296 (2021) 110465, <https://doi.org/10.1016/j.jfoodeng.2020.110465>.
- [41] A.A. Beldie, C.I. Moraru, Forward osmosis concentration of milk: product quality and processing considerations, *J. Dairy Sci.* 104 (2021) 7522–7533, <https://doi.org/10.3168/jds.2020-20019>.
- [42] C.A. Nayak, N.K. Rastogi, Forward osmosis for the concentration of anthocyanin from *Garcinia indica* Choisy, *Sep. Purif. Technol.* 71 (2010) 144–151, <https://doi.org/10.1016/j.seppur.2009.11.013>.
- [43] P.C.B.W. Mustika, W. Astuti, S. Sumardi, H.T.B.M. Petrus, I. Sutijan, Separation characteristic and selectivity of lithium from geothermal brine using forward osmosis, *J. Sustain. Metall.* 8 (2022) 1769–1784, <https://doi.org/10.1007/s40831-022-00602-z>.

Abbreviations

AL-FS: membrane's active layer facing the feed solution

BOD: five-day biochemical oxygen demand
COD: chemical oxygen demand
CP: concentration polarization
DO: dissolved oxygen
DS: draw solution
EC: electrical conductivity
EEM: excitation-emission matrix
FO: forward osmosis
FS: feed solution
LMH: liters per square meter per hour ($\text{L}\cdot\text{m}^{-2}\cdot\text{h}^{-1}$)
molMH: moles per square meter per hour ($\text{mol}\cdot\text{m}^{-2}\cdot\text{h}^{-1}$)
RSF: reverse solute flux
TN: total nitrogen
TOC: total organic carbon
TP: total phosphorus